Journal of
Nanoscience and Nanotechnology
Vol. 8, 5985–5992, 2008

Comparative Raman and HRTEM Study of Nanostructured GaN Nucleation Layers and Device Layers on Sapphire (0001)

P. Pant[1,*], J. Narayan[1], A. Wushuer[2], and M. H. Manghnani[2]

[1] Department of Materials Science and Engineering, Centennial Campus, North Carolina State University, Raleigh, NC 27695-7907, USA
[2] Hawai'i Institute of Geophysics and Planetology, University of Hawaii, Manoa, Honolulu, HI 96822, USA

Raman spectroscopy in conjunction with high-resolution transmission electron microscopy (HRTEM) has been used to study structural characteristics and strain distribution of the nanostructured GaN nucleation layer (NL) and the GaN device layer on (0001) sapphire substrates used for light-emitting diodes and lasers. Raman peaks corresponding to the cubic and the hexagonal phase of GaN are observed in the Raman spectrum from 15 nm and 45 nm NLs. A comparison of the peak intensities for the cubic and hexagonal phases of GaN in the NLs suggests that the cubic phase is dominant in the 15 nm NL and the hexagonal phase in the 45 nm NL. An increase in the density of stacking faults in the metastable cubic GaN (c-GaN) phase with increasing growth time lowers the system energy as well as locally converts c-GaN phase into hexagonal GaN (h-GaN). It also explains the observation of the more intense peaks of h-GaN in the 45 nm NL compared to c-GaN peaks. For the sample wherein an h-GaN device layer was grown at higher temperatures on the NL, narrow Raman peaks corresponding to only h-GaN were observed, confirming the high-quality of the films. The peak shift of the E_2^H(LO) mode of h-GaN in the NLs and the h-GaN film suggests the presence of a tensile stress in the NL which is attributed to defects such as stacking faults and twins, and a compressive stress in high-temperature grown h-GaN film which is attributed to the thermal-expansion mismatch between the film and the substrate. The peak shifts of the substrate also reveal that during the low temperature growth of the NL the substrate is under a compressive stress which is attributed to defects in the NL and during the high temperature growth of the device layer, there is a tensile strain in the substrate as expected from differences in coefficients of thermal expansion of the film and the substrate during the cooling cycle.

Keywords: GaN, Nucleation Layer, Raman Spectroscopy, Stress.

RESEARCH ARTICLE

1. INTRODUCTION

The growth of device quality GaN thin films by Metallorganic Chemical Vapor Deposition (MOCVD) and Molecular Beam Epitaxy (MBE) requires the deposition of a low-temperature (LT) ~550 °C nucleation layer (NL). The reduced growth temperature leads to the formation of a smoother layer on which device-quality GaN layer can be grown at higher-temperatures (HT) ~1050 °C.[1–3] The low-temperature (LT) growth of GaN results in a high nucleation density of the cubic GaN (c-GaN) phase. These nuclei grow epitaxially on (0001) sapphire substrate, but are slightly rotated ($\leq 1°$) with respect to each other. Upon coalescence of these epitaxial grains, subgrain boundaries are formed.[2,3] The edges of c-GaN provide a template for hexagonal GaN (h-GaN) growth at higher temperatures. It should be mentioned that c-GaN and h-GaN can be converted into each other via formation of stacking faults.[2,3] The NL has been shown to improve the crystalline quality of the film by promoting two-dimensional (2D) growth.[4,5] Despite the presence of a high density of defects in the NL, it provides a template for the subsequent growth of GaN and thus plays a crucial role in determining the quality of GaN device layers. Our earlier studies[2,3] focused on detailed High-Resolution Transmission Electron Microscopy (HRTEM) and X-ray diffraction studies of GaN nucleation layers (NLs) and device layers used for light-emitting diodes and lasers (LEDs and LDs). In this work, Raman spectroscopy which is a powerful non-destructive technique has been complemented with TEM and X-ray diffraction to fully reveal the details involving initial stages of the development of the NL. To our

*Author to whom correspondence should be addressed.

1533-4880/2008/8/5985/008 doi:10.1166/jnn.2008.334

knowledge no Raman studies have been reported on gallium nitride NLs and device layers. The present study represents a careful structural and microstructural study of the as-grown GaN nucleation layers and of the device layers for the fabrication of practical LEDs and LDs.

Cubic and hexagonal GaN are expected to have different lattice vibrations, which can be identified by Raman scattering measurements. Raman scattering of hexagonal wurtzite gallium nitride has been extensively studied.[6–10] The h-GaN which has a wurtzitic structure has eight sets of phonon modes, $(2A_1 + 2B_1 + 2E_1 + 2E_2)$ out of which one A_1, one E_1 and two E_2 are Raman active. Other A_1 and E_1 correspond to acoustic phonons and both B_1 modes are silent. The c-GaN, which has a zinc-blende structure, has a doubly degenerate TO (Transverse Optical) and a single LO (Longitudinal Optical) phonon with a higher frequency. Raman study on cubic GaN grown on (100) GaAs by MBE has been reported by Tabata et al.[11] In this work, we present a comparative study, using Raman spectroscopy and high-resolution TEM, of the as-grown GaN NLs of two different thicknesses (~15 nm and 45 nm) grown at low-temperature (~550 °C) and of the GaN device layer grown at higher-temperatures (~1050 °C) on the nucleation layer. The samples were all grown on (0001) sapphire substrate. The spectrum from the NLs contain Raman modes corresponding to both c-GaN as well as h-GaN, thus showing that the microstructure of the NL consists of both c-GaN and h-GaN phases. The spectrum from the h-GaN film grown at HT contains narrow well-defined h-GaN peaks, confirming high quality of the h-GaN films.

2. EXPERIMENTAL DETAILS

Comparative Raman spectroscopic and TEM studies were done on as-grown 15 nm and 45 nm thick NL. The study was also done on an h-GaN film grown on the NLs. The 514.5 nm line of an argon-ion laser was used as the excitation source for Raman scattering measurements. The spectra were recorded at room temperature in backscattering geometry with no polarization detection. The nucleation layers were grown on (0001) sapphire substrate using MOCVD growth technique by Kopin Corporation.[2] The (0001) sapphire substrates were cleaned with solvents and treated with flowing H_2 and NH_3 at 1100 °C. The NLs of varying thicknesses were grown at ~550 °C. The subsequent growth of GaN was carried out at 1050 °C to produce device quality h-GaN layers of optimal thickness for light-emitting diodes and laser diodes (LEDs and LDs) by Kopin Corporation.

3. RESULTS

3.1. Sapphire

For a reference, Raman spectrum from a pristine c-plane sapphire substrate was measured and the results are shown in Figure 1. The observed peaks for sapphire are at 418.01, 431.8, 448.8, 522.06, 577.17 and 750.36 cm^{-1}. Sapphire has two A_{1g} and five E_g modes which are Raman active.[12] Our measurements, which were taken in backscattering geometry, show the absence of the Raman modes at 378 cm^{-1} and at 645 cm^{-1}. These modes have been observed in the Raman spectrum of sapphire taken in several different orientations.[12] The sapphire peaks at ~418, 431, 448, 577, 748 cm^{-1} are also observed in the Raman spectrum of NL samples with thickness 15 nm and 45 nm, see Figures 2(a) and 3(a). For the h-GaN/NL/Sapphire sample sapphire modes are identified at 417.58 cm^{-1} and at 748.26 cm^{-1} in Figure 4.

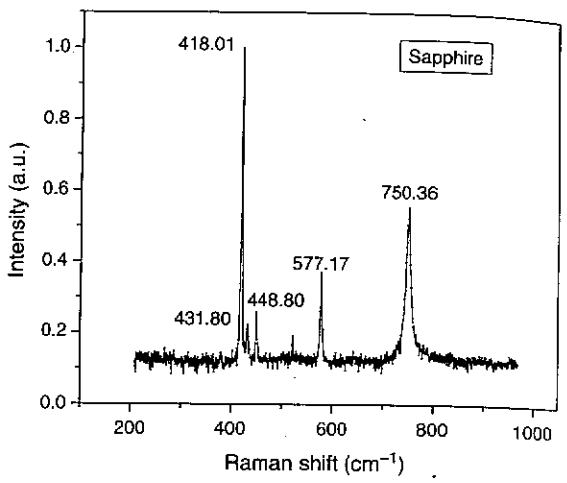

Fig. 1. (a) Raman spectrum from sapphire substrate taken at RT in backscattering geometry.

3.2. c-GaN (NL~15 nm)/Sapphire

Figure 2(a) shows the Raman spectrum of the sample with a NL thickness of ~15 nm grown on c-plane sapphire. The TO mode of c-GaN is observed at 553.27 cm^{-1} as can be seen clearly in the magnified plot in Figure 2(b). Figure 2(c) shows the magnified Raman spectrum from 720–770 cm^{-1}. A faint peak corresponding to the A_1(LO) mode of h-GaN is observed at 733.17 cm^{-1}. The sapphire peak at 748.75 cm^{-1} shows a shoulder peak at 739.40 cm^{-1} which could be due to the LO mode of c-GaN. A shoulder to the sapphire peak is also observed at 744.82 cm^{-1} and it could be attributed to the E_1(LO) mode of h-GaN. The presence of characteristic Raman peaks for c-GaN, h-GaN and sapphire in the range of 732 to 750 cm^{-1} causes overlapping of peaks, which requires a simulation model to interpret the contributions of the respective h-GaN and c-GaN phases to the peak.

3.3. c-GaN (NL~45 nm)/Sapphire

Figure 3(a) shows the Raman spectrum of the sample with a NL thickness of ~45 nm grown on c-plane sapphire.

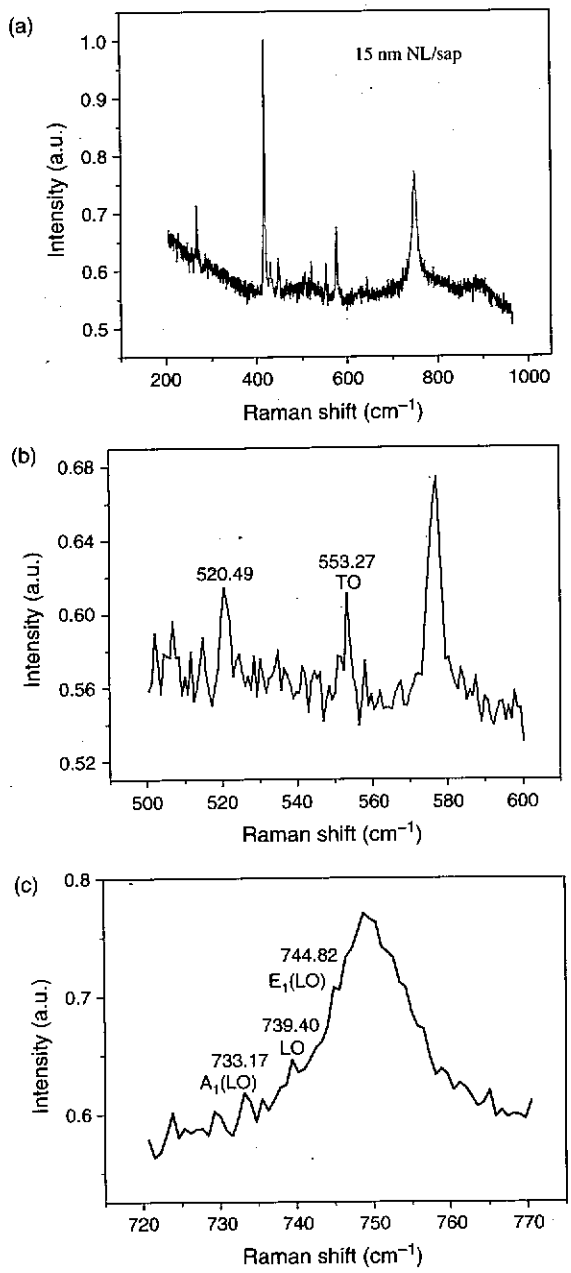

Fig. 2. (a) Raman spectrum from 15 nm NL/sap taken at RT in backscattering geometry using 514.5 nm wavelength for excitation. (b) Magnified plot from 500–600 cm^{-1} showing the TO mode of c-GaN. (c) Magnified plot from 720–770 cm^{-1} showing the A_1(LO) and E_1(LO) mode of h-GaN and the LO mode of c-GaN.

A peak corresponding to the E_2^H(LO) (higher frequency mode of E_2) mode of h-GaN is observed at 565.24 cm^{-1}, as marked in the magnified plot in Figure 3(b). A magnified Raman spectrum from 720–760 cm^{-1} is shown in Figure 3(c). The A_1(LO) mode of h-GaN is observed at 733.16 cm^{-1}. In addition, shoulder peaks to the sapphire peak at 749.52 cm^{-1} are also observed at 739.40 and 745.55 cm^{-1}. These peaks could be interpreted as contributions due to the LO mode of c-GaN and due to the E_1(LO) mode of h-GaN.

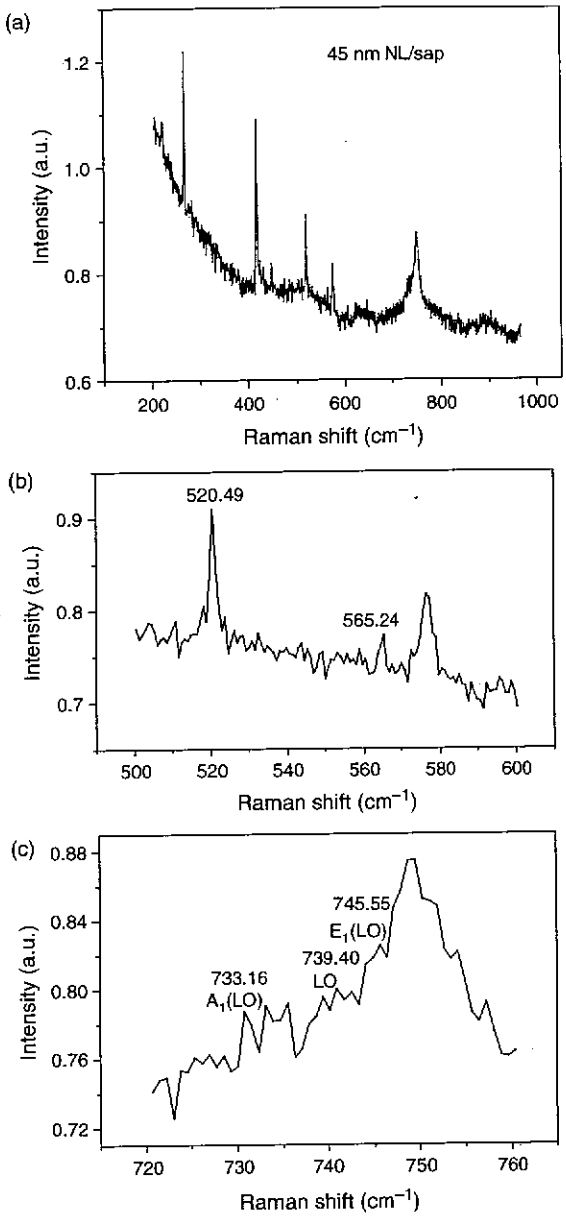

Fig. 3. (a) Raman spectrum from 45 nm NL/sap taken at RT in backscattering geometry using 514.5 nm wavelength for excitation. (b) Magnified plot from 500–600 cm^{-1} showing the E_2(LO) mode of h-GaN. (c) Magnified plot from 720–770 cm^{-1} showing the A_1(LO) and E_1(LO) mode of h-GaN and the LO mode of c-GaN.

3.4. Thick h-GaN/NL/Sapphire

Figure 4 shows Raman spectrum from a sample consisting of a thick h-GaN film grown on NL by MOCVD on c-plane (0001) sapphire substrate. The Raman spectrum from the h-GaN film shows peaks at 569.52, 734.24, and at 859.57 cm^{-1}. The peaks at 569.52 and 734.24 cm^{-1} are identified as the E_2^H(LO) and A_1(LO) modes of h-GaN. The E_2^H(LO) and A_1(LO) are the modes one would expect to observe for h-GaN in the backscattering configuration. The sharpness of these peaks suggests that the films are of good crystalline quality. The peak observed at 859.57 cm^{-1}

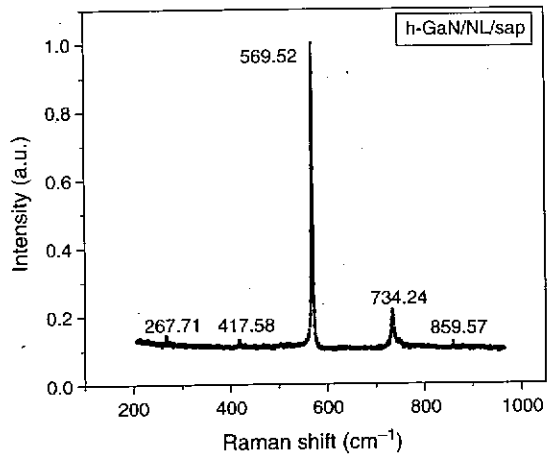

Fig. 4. Raman spectrum from the h-Gan/NL/sapphire sample showing the E_2(LO) and A_1(LO) mode of h-GaN.

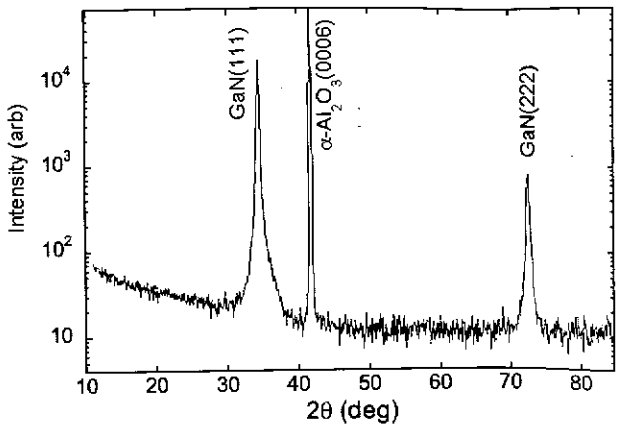

Fig. 5. A low-resolution X-ray θ–2θ scan along the Al_2O_3 [0001] substrate with a logarithmic scale for the 45 nm NL.

is not a first order Raman peak, but has been identified[13] as a second-order Raman mode (855 cm^{-1}) of h-GaN having A_1, E_1 and E_2 symmetry. The second-order Raman spectrum can be observed if the film quality is very good. Siegle et al.[13] have attributed the mode at 855 cm^{-1} to a second-order Raman scattering processes resulting from a combination of acoustic and optical phonons. In second-order Raman scattering the conservation rule requires that the sum of the wave-vectors of the two phonons participating in the Raman scattering be zero. Therefore, the phonon modes in second-order Raman scattering are not limited to those at Γ point unlike the first-order scattering, but extend to the whole Brillouin zone. The sharp peak at 268 cm^{-1} is not a theoretically predicted peak for either sapphire or h-GaN or c-GaN. Foreign signals with sharp peaks observed in Raman spectra have been attributed either to the presence of impurity atoms or to the presence of defects such as vacancies.[9]

4. DISCUSSION

Structural information about the GaN NL characteristics has been studied in detail by HRTEM and X-ray diffraction in our earlier works.[2–3] Because the NL is very thin, a low resolution θ–2θ scan from a nucleation layer/sapphire sample in Figure 5 shows intense Al_2O_3 (0006) peaks from the substrate and less intense c-GaN (111) and (222) peaks from the NL. The results of θ–2θ scans through c-GaN (111) peaks in conjunction with Φ scans showed the alignment of c-GaN (111)//Al_2O_3 (0001) planes in addition to other basal planes.[3] By measuring $\Delta\theta$ (FWHM) the average misorientation between the subgrains was found to be ~1.3°. Low resolution L-scans (10L in hexagonal coordinates) and modeling calculations showed that the NL had 63% of c-GaN phase and 37% of h-GaN.[3] In our earlier work[2] we have shown that the NL grows epitaxially aligned with sapphire substrate via domain matching epitaxy.

A qualitative comparison of the Raman peak intensities for the cubic and hexagonal phases of GaN in the 15 nm and 45 nm NLs suggests that the cubic phase is more abundant in the 15 nm NL and the hexagonal phase in the 45 nm NL. Detailed studies[1–3,14,15] have shown that at low temperatures ~530–600 °C the GaN NL which grows epitaxially via Volmer-Weber (island) growth mode, is single crystal but contains low-angle (subgrain) boundaries. Conventional and HRTEM studies done by us earlier[2] have shown that the as-grown NL has a cubic structure and contains a high density of defects including stacking faults, twins and low angle grain boundaries. The low-magnification images of the GaN NL in Figures 6(a and b) indicate the presence of defects such as stacking faults and low-angle subgrain boundaries. The high-resolution images in Figures 7(b and c) show explicitly the presence of {111} stacking faults. It is well known that there are four orientations for the {111} planes in c-GaN. From the HRTEM images it is seen that during initial stages of growth, stacking faults in one set of planes in c-GaN dominate leading to different types of grains containing low-angle grain boundaries. The formation of c-GaN during low temperature growth of the NL has been attributed to nitrogen deficiency resulting from insufficient pyrolysis of ammonia at low temperatures.[16] However, c-GaN is a metastable phase of higher energy and therefore can lower its energy by introducing stacking faults and transforming into the lower energy equilibrium h-GaN phase. This transformation from c-GaN to h-GaN at LT growth has been elucidated previously.[2] The localized regions of faulted c-GaN can be regarded as localized regions of hexagonal GaN (h-GaN). The formation of c-GaN at low substrate temperatures and subsequent lowering of energy of the system by insertion of stacking faults leading to formation of h-GaN locally, explains the simultaneous observation of the c-GaN and h-GaN Raman modes in the 15 nm and 45 nm NLs.

During the initial stages of growth, the NL (~15 nm) is predominantly cubic with a very small fraction of h-GaN

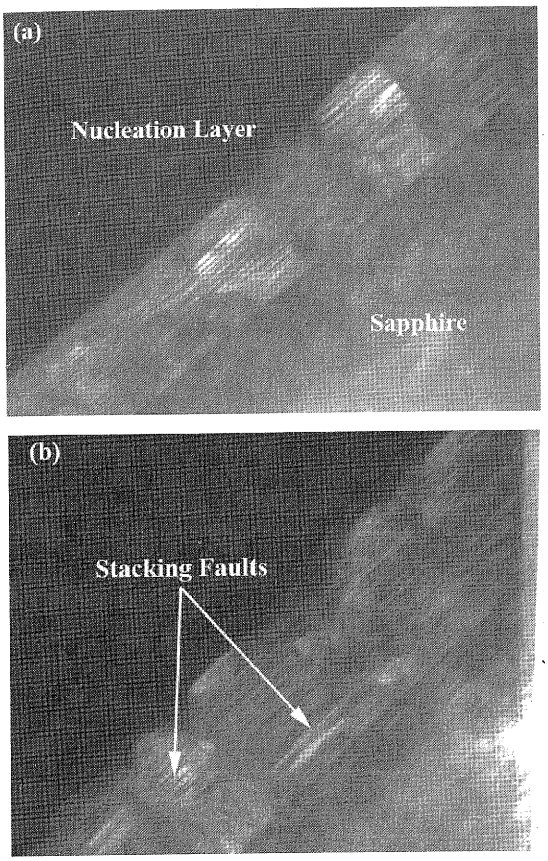

Fig. 6. (a) Cross-section TEM micrograph along {110} c-GaN and {1010} sapphire showing the NL and the sapphire substrate at low magnification. (b) The c-GaN subgrains contain stacking faults in different {111} planes and the unfaulted grains are separated by low-angle subgrain boundaries.

or stacking fault induced disorder present in the NL. As reported earlier[2–3] by our group, the localized transformation of c-GaN into h-GaN during growth of the NL restrains the growth of the unfaulted c-GaN and leads to formation of the more stable phase of GaN, that is the faulted c-GaN phase (or h-GaN) locally, thereby giving grains containing mainly faulted c-GaN or h-GaN regions and very few regions of unfaulted c-GaN. This explains the presence of well defined $E_2^H(LO)$ mode (565.24 cm^{-1}) of h-GaN in the 45 nm NL. The observation of the well defined peaks of the LO mode of c-GaN, $A_1(LO)$ mode and $E_1(LO)$ mode of h-GaN is obscured for the 15 nm and 45 nm NL samples due to the overlapping of peaks of c-GaN, h-GaN and sapphire in the range of 733–750 cm^{-1}. The TO mode in c-GaN and the $E_1(LO)$ mode in h-GaN are forbidden modes in backscattering geometry but are observed in the Raman spectra of the NLs. Tabata et al.[11] have reported the appearance of the forbidden TO mode of c-GaN which they explained as being due to short range perturbations. It is known that presence of disorder in the lattice breaks the Raman selection rules of phonon momentum conservation, $q = 0$. The resultant relaxation of phonon momentum conservation allows the

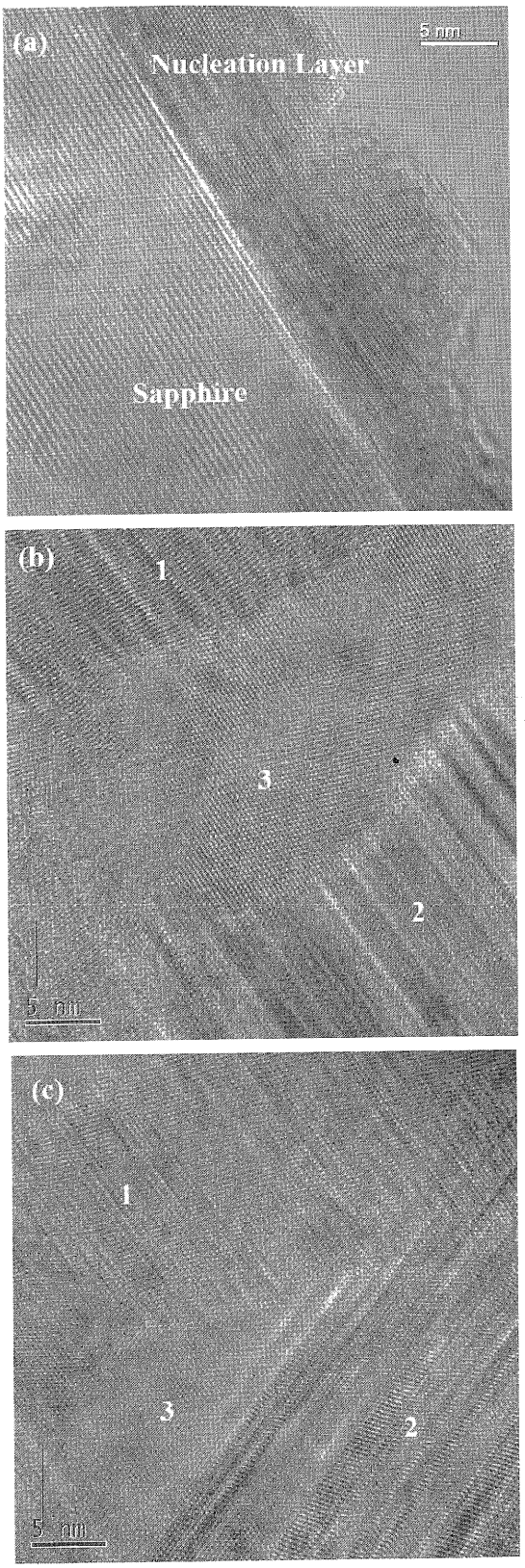

Fig. 7. High-resolution cross-section TEM micrograph along {110} c-GaN and {1010} sapphire showing (a) the NL and the sapphire substrate interface region (b), (c) the faulted c-GaN grains (1 and 2) and unfaulted c-GaN grain (3). The contrast in the images arises from the presence of stacking faults in different {111} planes.

forbidden modes to be observed in the Raman spectrum. Another point of interest in these spectra is the observation of the TO mode (553.27 cm^{-1}) of c-GaN using the 514.5 nm laser wavelength for excitation. Interestingly, in the works of Tabata et al.[11] the TO mode was not observed when the 514.5 nm wavelength was used to excite the c-GaN/(001)GaAs sample, but it was observed when the spectrum was taken at shorter wavelengths (488 nm and 457.9 nm). The samples used in their study were grown by MBE on (001) GaAs substrate and such samples have been found to have a much lower density of defects such as stacking faults, twins and point defects as shown by Strite et al.[17] In the present work, the samples were grown by MOCVD on (0001) sapphire substrate at a lower temperature, which leads to a much higher defect content.

An interesting feature of the Raman spectra from the h-GaN film and the NLs (15 nm and 45 nm) is the observation of peaks at ~268 cm^{-1} and at ~520 cm^{-1}. These peaks have not been previously observed in Raman spectrum of c-GaN or h-GaN phases under normal growth conditions. Neither h-GaN nor c-GaN has any predicted Raman modes at 268 cm^{-1}. The contribution of the substrate towards the mode at ~268 cm^{-1} is ruled out since Raman spectrum from sapphire substrate in Figure 1 does not show this mode. The narrow nature of the peak in the NLs and the h-GaN/NL/sap samples suggests that the origin of the peak could be due to discrete defects such as vacancies and/or SFs in the NL in the present case. Stacking Faults (SFs) and point defects have discrete energy levels associated with them. Because of their discrete energy levels in the lattice it is presumed that the peaks related to SFs and point defects would be narrow peaks. It is known that insufficient pyrolysis of NH_3 during LT growth of NL gives rise to nitrogen vacancies which in turn promote the growth of the metastable c-GaN phase. The defect concentration is expected to increase with increasing thickness of the NL, which could also explain the observation that on a relative scale the peak intensity at 268 cm^{-1} is maximum for the 45 nm NL. A comparison of the peak observed at ~520 cm^{-1} in Figures 3(a) and 2(a) show that the peak is more intense in the 45 nm NL, and is less intense in the 15 nm NL. The sapphire substrate shows a peak at 522 cm^{-1}. Since neither sapphire nor h-GaN nor c-GaN has a characteristic peak around 520 cm^{-1}, we suggest that these peaks could be caused by the laser (natural emission) in sapphire. Tabata et al.[11] have also reported on the observation of a small peak at 512 cm^{-1} in the Raman spectrum of c-GaN grown on GaAs.

5. STRESSES IN FILMS AND SUBSTRATE

The E_2^H(LO) phonon frequency in h-GaN has a nonpolar character and shifts linearly with stress. Therefore, it has been used by several groups[18–21] to measure biaxial stress in GaN epilayers. The E_2^H(LO) phonon frequency of unstrained GaN is reported at 567 cm^{-1}.[22] A decrease in the value of the E_2^H(LO) phonon frequency with respect to that of unstrained GaN indicates tensile stress and an increase in the E_2^H(LO) phonon frequency indicates compressive stress. The E_2^H(LO) mode is observed at 565.24 cm^{-1} in the 45 nm NL. The shift in the E_2^H(LO) phonon frequency towards lower frequency indicates that the GaN NL is under tensile stress. This conclusion is supported by our earlier work[3] where high resolution X-ray scans of the NL found the presence of tensile stress in the NL. From our studies we conclude that the presence of defects such as twins and stacking faults and the strain fields around them due to missing half planes give rise to the observed tensile stress in the NL. The tensile stress generated due to defects seems to dominate the stress due to thermal expansion mismatch between the NL and the substrate which is expected to be compressive in the NL as shown by our calculations in Table I. Interestingly, for the h-GaN film grown on NL, the E_2^H(LO) mode is observed at 569.52 cm^{-1} thereby indicating a compressive biaxial stress in the film, which is consistent with thermally induced strains between h-GaN and sapphire. The difference of thermal coefficient of expansion of h-GaN ($\alpha_a = 5.59\times10^{-6}$/K, $\alpha_c = 3.17\times10^{-6}$/K)[24] and sapphire ($\alpha_a = 7.5\times10^{-6}$/K, $\alpha_c = 8.5\times10^{-6}$/K)[25] is expected to lead to compressive strain upon cooling from a high-temperature growth. Intensive high-resolution TEM studies of GaN films grown on nucleation layer have shown that though the film has dislocations, it is free of defects like twins and stacking faults. In the absence of these defects, the thermal expansion mismatch compressive stress dominates in the film grown on the NL and it manifests itself as a frequency shift of the E_2^H(LO) mode of h-GaN towards high frequency.

Table I. Calculated stress in the film and the parameters used to calculate stress.

	c-GaN	h-GaN	Sapphire
Thermal coefficient of expansion (K^{-1})	3.5×10^{-6} [23]	5.59×10^{-6} [24]	7.5×10^{-6} [25]
Poisson's ratio	0.352[a]	0.17[a]	0.25[c]
Young's modulus (GPa)	181.137[a]	290[b]	352[c]
Calculated residual stress ($\Delta T = 523$ K)	−0.584	−0.362	
Calculated residual stress ($\Delta T = 1023$ K)	—	−0.708	

[a]Values of elastic constants taken from Ref. [26]. [b]Ref. [27]. [c]Ref. [28].

Table II. Shift observed in the Raman peak of sapphire.

Sapphire peak	cm^{-1}
Bare sapphire substrate	418.01
15 nm NL/sap	418.09
45 nm NL/sap	418.09
h-GaN/NL/sap	417.58

Another related interesting observation in this study was the shift observed in the sapphire substrate peaks at ~418 cm^{-1} and at 750 cm^{-1} for the samples under study. Table II lists the sapphire peaks at ~418 cm^{-1} recorded from a bare sapphire substrate, 15 nm NL, 45 nm NL and h-GaN/NL/sapphire samples. The peak shift indicates the presence of stress in the substrate. It is observed that during LT growth (15–45 nm, ~550 °C) the peak shift for the substrate is towards higher frequencies and, though small, it indicates a compressive stress in the substrate. In contrast, for the HT growth (~500 nm, 1050 °C) there is a considerable peak shift towards low frequency which indicates a tensile stress in the substrate. The observation of a small shift in the sapphire peak towards higher frequencies for the NL samples combined with our earlier observation of a shift towards lower frequencies of the E_2^H(LO) mode of h-GaN for the same samples leads to the conclusion that during LT growth of the NL, the stress due to defects dominates over the thermal expansion mismatch stress. Though most of the stress due to the defects in the NL is confined to the film only because of its small thickness, the sapphire substrate peak shift suggests that a small amount of the stress also appears across the interface in the substrate thereby explaining the observed compressive stress in the substrate during LT growth. In the case of HT growth, there is a considerable shift in the sapphire peak towards low frequency and a corresponding shift of the E_2^H(LO) mode of h-GaN towards higher frequencies. Post-growth cooling of the samples from growth temperatures (1050 °C) to room temperature, results in a compressive stress in the film and a tensile stress (opposite character) in the substrate due to differences in the thermal coefficients of expansion of the film and the substrate. The in-plane thermal coefficient of expansion of sapphire (7.5×10^{-6}/K) is greater than that of h-GaN (5.59×10^{-6}/K). Therefore, sapphire contracts at a much faster rate than h-GaN on cooling from the growth temperature to room temperature which in turn causes a residual tensile stress in the sapphire substrate and a compressive stress in the film. The tensile strain in the sapphire substrate manifests as a frequency shift towards low frequency as listed in Table II. The calculated stress values in the film and the parameters used for stress calculation are listed in Table II. The above stress determinations for the sapphire substrate were made using the 418 cm^{-1} peak shifts. The peak at 750 cm^{-1} was not used since the existence of other overlapping peaks in the range 733–750 cm^{-1} makes it difficult to determine a precise value of shift.

6. CONCLUSION

We have investigated the structure of GaN NLs of different thicknesses and of GaN device layers. The growth were done on (0001) sapphire substrate by MOCVD. Analysis of the Raman modes observed in the 15 nm and 45 nm NLs, and h-GaN/NL/sap samples shows that the NL contains both the c-GaN and h-GaN phases; and the h-GaN film contains only the h-GaN phase. The presence of stronger Raman modes of c-GaN compared to the weaker modes of h-GaN in the 15 nm NL suggests that during initial stages of growth the GaN NL has a predominantly cubic character with a very small percentage of h-GaN phase present. With increase in growth time of the NL (~45 nm) it is seen that the h-GaN Raman modes become more intense compared to the c-GaN modes, indicating that the 45 nm NL has a higher fraction of faulted c-GaN (or h-GaN) present. Qualitative interpretations of the E_2^H(LO) mode shift of h-GaN as observed in the Raman spectrum of the 15 nm, 45 nm NLs and h-GaN/NL/sapphire samples indicates the presence of a tensile stress in the NL and a compressive stress in the h-GaN film. These Raman results are in a complete agreement with X-ray diffraction and HRTEM results on defects and epitaxial nature of thin films. The shift in the sapphire peaks indicates that the presence of defects such as SFs and twins in the NL causes a tensile stress in the NL and a compressive stress in the substrate. The stress due to defects actually dominates over the compressive thermal stress that is predicted due to the thermal-coefficient of expansion (TEC) mismatch of the NL with the substrate. In contrast, the h-GaN films grown at higher-temperatures (~1050 °C) that are free of such defects, show the onset of a compressive stress and the substrate exhibits a complementary tensile stress due to TEC mismatch between GaN and sapphire substrate. Thus, the misfit stress is confined primarily to the film during initial stages of growth and as the film thickness increases, the stress is increasingly shared by the substrate.

RESEARCH ARTICLE

References and Notes

1. V. Narayanan, K. Lorenz, W. Kim, and S. Mahajan, *Phil. Mag. A* 82, 885 (**2002**).
2. J. Narayan, P. Pant, A. Chugh, H. Choi, and J. C. C. Fan, *J. Appl. Phys.* 99, 054313 (**2006**).
3. J. Narayan, P. Pant, W. Wei, R. J. Narayan, and J. D. Budai, *J. Nanosci. Nanotechnol.* 7, 2719 (**2007**).
4. S. Yoshida, S. Misawa, and S. Gonda, *J. Vacc. Sci. and Techn. B* 1, 250 (**1983**).
5. H. Amano, N. Sawaki, I. Akasaki, and Y. Toyoda, *Appl. Phys. Lett.* 48, 353 (**1986**).
6. G. Burns, F. Dacol, J. C. Marinace, B. A. Scott, and E. Burstein, *Appl. Phys. Lett.* 22, 356 (**1973**).
7. A. Cingolani, M. Ferrara, M. Lugará, and G. Scamarcio, *Sol. State Commun.* 58, 823 (**1986**).
8. P. Perlin, C. J. Carillon, J. P. Itie, A. S. Miguel, I. Grzegory, and A. Polian, *Phys. Rev. B* 45, 83 (**1992**).

9. H. Harima, *J. Phys.: Condens. Matter.* 14, R967 (**2002**).
10. T. Azuhata, T. Matsunaga, K. Shimada, K. Yoshida, T. Sota, K. Suzuki, and S. Nakamura, *Phys. B* 219&220, 493 (**1996**).
11. A. Tabata, R. Enderlein, J. R. Leite, S. W. da Silva, J. C. Galzerani, D. Schikora, M. Kloidt, and K. Lischka, *J. Appl. Phys.* 79, 4137 (**1996**).
12. S. P. S. Porto and R. S. Krishnan, *J. Chem. Phys.* 47, 1009 (**1967**).
13. H. Siegle, G. Kaczmarczyk, L. Filippidis, A. P. Litvinchuk, A. Hoffmann, and C. Thomsen, *Phys. Rev. B* 55, 7000 (**1997**).
14. X. H. Wu, P. Fini, S. Keller, E. J. Tarsa, B. Heying, U. K. Mishra, S. P. DenBaars, and J. S. Speck, *Jpn. J. Appl. Phys.* 35, L1648 (**1996**).
15. P. Vennegues, B. Beaumont, M. Vaille, and P. Gibart, *J. Cryst. Growth* 173, 249 (**1997**).
16. S. Oktyabrsky, K. Dovidenko, A. K. Sharma, J. Narayan, and V. Joshkin, *Appl. Phys. Lett.* 74, 2465 (**1999**).
17. S. Strite, J. Ruan, N. Manning, A. Salvador, H. Chen, D. J. Smith, W. J. Choyke, and H. Morkoc, *J. Vac. Sci. Technol. B* 9, 1924 (**1991**).
18. C. Kisielowski, J. Krüger, S. Ruvimov, T. Suski, J. W. Ager, III, E. Jones, L. Weber, M. Rubin, E. R. Weber, M. D. Bremser, and R. F. Davis, *Phys. Rev. B* 54, 17745 (**1996**).
19. T. Kozawa, T. Kachi, H. Kano, H. Nagase, N. Koide, and K. Manabe, *J. Appl. Phys.* 77, 4389 (**1995**).
20. I. Lee, I. Choi, C. Lee, E. Shin, D. Kim, S. K. Noh, S. Son, K. Lim, and H. J. Lee, *J. Appl. Phys.* 83, 5787 (**1998**).
21. M. Kuball, *Surf. Interface Anal.* 31, 987 (**2001**).
22. V. Yu. Davydov, Yu. E. Kitaev, I. N. Goncharuk, A. N. Smirnov, J. Graul, O. Semchinova, D. Uffmann, M. B. Smirnov, A. P. Mirgorodsky, and R. A. Evarestov, *Phys. Rev. B* 58, 12899 (**1998**).
23. D. N. Talwar, *Appl. Phys. Lett.* 80, 1553 (**2002**).
24. H. P. Maruska and J. J. Tietjen, *Appl. Phys. Lett.* 15, 327 (**1969**).
25. M. Leszczynski, T. Suski, H. Teisseyre, P. Perlin, I. Grzegory, J. Jun, S. Porowski, and T. D. Moustakas, *J. Appl. Phys.* 76, 4909 (**1994**).
26. A. F. Wright, *J. Appl. Phys.* 82, 2833 (**1997**).
27. S.-R. Jian, T.-H. Fang, and D.-S. Chuu, *J. Electron. Mater.* 32, 496 (**2003**).
28. L. Liu and J. H. Edgar, *Mater. Sc. Engr. R* 37, 61 (**2002**).

Received: 13 January 2008. Revised/Accepted: 6 February 2008.